

## SECONDARY CELLS WITH LITHIUM ANODES AND IMMOBILIZED FUSED-SALT ELECTROLYTES

H. Shimotake, G. L. Rogers, and E. J. Cairns

Argonne National Laboratory  
9700 South Cass Avenue  
Argonne, Illinois  
60439

### Introduction

Today's rapidly-advancing technology requires a wide spectrum of power sources and energy-storage devices. In many applications, the power sources are required to have a minimum size or weight per unit of power or energy. These requirements have motivated a great deal of the recent work on high-specific-energy (watt-hr/lb) and high-specific-power (watt/lb) secondary cells. The maximization of the specific energy requires that reactants of low equivalent weight and high free energy of reaction be used. For high specific energy ( $> 50$  watt-hr/lb) cells with aqueous electrolytes, zinc and cadmium have served as anode materials while nickel oxide, silver oxide, and oxygen (or air) have served as cathode materials.<sup>1,2,3</sup> The elimination of water from the electrolyte permits more reactive metals such as calcium and the alkali metals to be considered as anode materials. Lithium has a very low equivalent weight and low electronegativity, making it particularly attractive as an anode material for high specific energy cells. A number of cathode materials have been used in combination with nonaqueous electrolytes and lithium anodes, depending on the operating temperature and the electrolyte.

Lithium-anode cells designed for operation at room temperature use non-aqueous electrolytes comprised of solutions of inorganic salts such as  $\text{LiPF}_4$  or  $\text{LiClO}_4$  dissolved in organic solvents such as propylene carbonate or dimethyl sulfoxide; the cathodes are usually metal halides such as  $\text{NiF}_4$ ,  $\text{CuF}_2$  or  $\text{CuCl}$ .<sup>1,3</sup> Although these cells have the potentiality of supplying over 100 watt-hr/lb at low discharge rates, their specific power is low (2-20 watt/lb),<sup>1,3</sup> limiting their range of applicability. The specific power for cells with organic-solvent electrolytes is low because of the low conductivity of the electrolyte ( $\sim 10^{-2} \text{ ohm}^{-1} \text{ cm}^{-1}$ ).

The use of fused-salts as electrolytes provides very high conductivities ( $1\text{-}4 \text{ ohm}^{-1} \text{ cm}^{-1}$ ) thus allowing specific powers in excess of 100 watt/lb to be achieved.<sup>4-8</sup> Because of their relatively high melting points, fused-salt electrolytes require elevated operating temperatures ( $260\text{-}650^\circ\text{C}$ ). A number of secondary cells with fused-salt electrolytes have been investigated, including sodium/bismuth,<sup>9</sup> lithium/chlorine,<sup>7,8</sup> lithium/tellurium,<sup>4-6</sup> and lithium/selenium,<sup>10</sup> all using free liquid electrolytes.

A general indication of the theoretical maximum specific energies of some couples suitable for use with fused-salt electrolytes is given in Figure 1, where the specific energy (as calculated from the equivalent weight of the cell products indicated and the average emf of the couple) is plotted against the equivalent weight of the active material. Usually, the higher specific energy materials are more difficult to handle from a corrosion viewpoint.

A great deal of design flexibility and compactness can be gained by immobilizing the fused-salt electrolyte either in an absorbent matrix or in the form of a rigid paste.<sup>11-13</sup> This work deals with secondary cells having liquid lithium anodes, liquid bismuth or tellurium cathodes and fused-lithium-halide electrolytes immobilized as a rigid paste, operating at temperatures in the range  $380$  to  $485^\circ\text{C}$ .

### Experimental

Typical lithium/bismuth and lithium/tellurium cells are shown in Figures 2 and 3. The cell housing in Figure 2 was made from Type 316 stainless steel; the electrode compartments were 3.2 mm deep, and had 4 concentric fins which

served as current collectors. The exposed electrolyte area was  $1.98 \text{ cm}^2$ , and the paste electrolyte thickness was  $0.34 \text{ cm}$ . Prior to assembly, the anode compartment was loaded with  $0.064 \text{ gm}$  of lithium (Foote Mineral Co.,  $0.003\% \text{ Na}$ ,  $0.003\% \text{ K}$ ,  $0.003\% \text{ N}_2$ ,  $0.003\% \text{ Cl}_2$ , surface oxide removed), heated to  $530^\circ\text{C}$  to ensure good wetting of the current collector. The cathode compartment contained  $2.764 \text{ gm}$  of bismuth (United Mineral and Chemical Corp.,  $99.999\%$  minimum purity). These amounts of reactants correspond to a cathode-alloy composition of  $41 \text{ a/o Li in Bi}$  at complete discharge, and a cell capacity of  $0.25 \text{ amp-hr}$ . The cell was prepared and assembled under a high-purity helium atmosphere.<sup>14</sup> No gaskets were used; the smooth-surfaced electrolyte disc provided a leak-tight seal against the cell housing.

The lithium/tellurium cell, made of pure iron, had current collectors consisting of sheets of sintered porous stainless steel in the anode compartment, and a network of pure-iron wires in the cathode compartment in place of the meshes shown in Figure 3. The exposed electrolyte area was  $3.25 \text{ cm}^2$ ; the electrolyte thickness was  $0.32 \text{ cm}$ . The cell compartments were loaded with  $0.75 \text{ gm}$  of lithium and  $5.45 \text{ gm}$  of tellurium, (American Smelting and Refining Co.,  $99.999\%$  minimum purity) corresponding to  $71.6 \text{ a/o Li in Te}$  at complete discharge.

The electrolyte was the ternary eutectic composed of  $11.7 \text{ m/o LiF}$  -  $29.1 \text{ m/o LiCl}$  -  $59.2 \text{ m/o LiI}$ , which melts at  $340.9^\circ\text{C}$  and has a specific conductance of  $2.3 \text{ ohm}^{-1} \text{ cm}^{-1}$  at  $375^\circ\text{C}$  and  $3.0 \text{ ohm}^{-1} \text{ cm}^{-1}$  at  $475^\circ\text{C}$ .<sup>15</sup> The eutectic was prepared from weighed amounts of the pure salts:  $\text{LiF}$ ,  $\text{LiCl}$ , and  $\text{LiI}$  all supplied by Anderson Physics Laboratories, Inc. After the components were melted together to form the eutectic, the electrolyte was solidified, pulverized to  $-300$  mesh, and mixed ( $50 \text{ w/o}$ ) with an inert filler material. The electrolyte-filler powder mixture was then molded into discs. For the  $\text{Li/Bi}$  cell, discs  $1.85 \text{ cm}$  in dia. were prepared by pressing the electrolyte-filler powder first at room temperature to form "cold-pressed" discs, and then at  $400^\circ\text{C}$  for final densification. All operations except for the hot-pressing were carried out in a pure helium atmosphere. For the  $\text{Li/Te}$  cell, discs  $2.5 \text{ cm}$  in dia. were pressed at room temperature and sintered at  $400^\circ\text{C}$  without pressing, eliminating all exposure to air.

The paste electrolyte has a continuous phase of fused-lithium-halide eutectic at the cell operating temperature. The relative amounts of finely-divided inert filler and lithium halide are chosen such that the electrolyte fills the interstitial spaces among the very small filler particles, and holds the paste firmly by means of its high surface tension, low contact angle with the filler, and the small pore size of the compact. Similar paste electrolytes have been used with success in molten-carbonate fuel cells.<sup>11-13</sup>

The measurements of cell performance were carried out with the aid of a constant-current DC power supply, precision voltmeters and ammeters ( $1/4$  percent), and a strip-chart recorder. The voltage-current density curves for the discharge mode of operation were measured starting with the cell in the fully-charged condition; the curves for the charge mode of operation were usually measured from the fully-discharged condition. All results are reported on a resistance-included basis. The cells were held at operating temperature in an electrically-heated tube furnace.

### Results and Discussion

The voltage-current density curves for the  $\text{Li/Bi}$  cell operating at  $380^\circ$ ,  $453^\circ$ , and  $485^\circ\text{C}$  are shown in Figure 4. As might be expected, the highest performance in both charge and discharge modes was obtained at the highest temperature. Current densities up to  $2.2 \text{ amp/cm}^2$  were obtained, based on the effective electrode area of  $1 \text{ cm}^2$  (the electrode compartments were only about half-filled with active materials during these experiments). Since the cathode composition during the discharge experiments averaged about  $5 \text{ a/o Li}$ ,<sup>16</sup> these performances are typical of those obtainable near the beginning of the plateau of the corresponding voltage-

time curves at constant current discharge. The maximum power density at 485°C was 0.57 watt/cm<sup>2</sup> at 0.6 volt.

The slopes of the charge and discharge curves in Figure 4 are different because of the difference in state of charge for the two modes of operation. The internal resistance of the cell is expected to be lower for the discharge curves because most of the original amount of lithium was still in the anode compartment when the discharge data were taken. During the charging experiments, however, almost no lithium was present in the lithium compartment, resulting in a relatively high internal resistance. When charge and discharge curves are taken under identical conditions, the curves have the same slope. The internal resistance of the cell at high current densities was 0.45 ohm at 485°C, compared to a value of 0.23 ohm calculated from the specific conductance of the electrolyte and a paste-to-pure electrolyte resistivity ratio of 2.11,<sup>13</sup> This discrepancy could be caused by the presence of some Li<sub>2</sub>O resulting from hydrolysis of the lithium halides during hot-pressing or incomplete wetting of the paste by Li.

From the reasonably high current density capabilities of the Li/Bi cell of Figure 4, it is clear that the cell can be fully charged from complete discharge in about 15 minutes.

The performance characteristics of the (larger) Li/Te cell operating at 475°C are shown in Figure 5. As expected on the basis of the emf measurements of Foster and Liu<sup>17</sup> and earlier experience with Li/Te cells,<sup>4-6</sup> the open circuit voltage was 1.7 to 1.8 volts, and the voltage-current density curves were straight lines, indicating the absence of any significant concentration or activation over-voltages. The short-circuit current density was 2.2 amp/cm<sup>2</sup>, and the maximum power density was 1 watt/cm<sup>2</sup> at 0.9 volt, a considerable improvement in power density over the Li/Bi cell.

The internal resistance of the Li/Te cell during discharge was 0.24 ohm, compared to 0.065 ohm calculated from the electrolyte conductivity and a paste-to-pure electrolyte resistivity ratio of 2. The ratio of observed-to-calculated cell resistances is higher for the Li/Te cell than for the Li/Bi cell, possibly because of the fact that the paste electrolyte disc for the Li/Te cell was not hot-pressed, and therefore probably contained voids which increased the resistivity of the paste.

The Li/Te cell, with a capacity of 2.91 amp-hr could be fully charged from complete discharge in less than half an hour. This is a much higher charge rate than can be used with secondary cells having aqueous electrolytes or cells with nonaqueous organic solvent electrolytes.

Extensive investigations of constant-current charge and discharge characteristics, charge retention, and cycle life still remain to be done. The data presented above were interesting enough, however, that some preliminary design calculations have been performed, based upon the voltage-current density curves of Figures 4 and 5.

The principles, equations, and sample calculations involved in the design of secondary batteries have already been discussed elsewhere<sup>4</sup>, therefore, no detailed explanations will be given here. The most important parameter in many applications is battery weight; therefore, the energy and power values are expressed per unit weight as specific energy (watt-hr/lb) and specific power (watt/lb). The calculation of battery weight involves the selection of the ratio of reactant weights, and the calculation of the weights of reactants, electrolyte, cell housing, terminals, etc. required, per unit of active cell area. The specific power available is calculated from the current density-voltage curve and the battery weight per unit active area. The specific energy is calculated from the average cell operating voltage, the amount of lithium per unit of active cell area and the battery weight per unit of active area.<sup>4</sup> The values used in these calculations are summarized in Table I.

#### 4.

The results of the design calculations for Li/Bi and Li/Te secondary batteries are shown in Figure 6. Because of the lower equivalent weight and higher electronegativity, the Li/Te cell has higher specific energy and specific power capabilities than the Li/Bi cell. As an example, Figure 6 shows that for the 30-minute-discharge rate, a Li/Bi cell having 3 cells per inch and an electrolyte thickness of 0.32 cm has a specific power of 43 watt/lb and a specific energy of 21 watt-hr/lb, whereas the Li/Te cell of similar dimensions can attain 110 watt/lb and 55 watt-hr/lb. The design analysis results presented in Figure 6 also indicate that if the electrolyte thickness is decreased to 0.1 cm, it is possible to achieve 90 watt/lb and 45 watt-hr/lb for the Li/Bi cell and 200 watt/lb and 110 watt-hr/lb for the Li/Te cell. The performances of some other types of secondary batteries including lead-acid, nickel/cadmium, sodium/sulfur, and lithium/chlorine are presented in Figure 6 for comparison.

Possible applications for secondary cells with the characteristics of the Li/Te cell include space power sources, military communications power sources, military vehicle propulsion, and perhaps special commercial vehicle propulsion.<sup>5</sup>

The areas which deserve further attention in the development of Li/Bi and Li/Te cells include the optimization of paste electrolyte properties (particularly the resistivity), current collection, corrosion, cycle life, and thermal cycling.

#### Conclusions

1. It is possible to form acceptable paste electrolytes from fused-lithium halides and inert filler materials. The paste electrolytes presently show two to three times the expected electrolytic resistivities.

2. Lithium/bismuth and lithium/tellurium cells operating with lithium halide paste electrolytes can operate at power densities of 0.57 and 1.0 watt/cm<sup>2</sup>, respectively at about 480°C.

3. These cells can be charged at very high rates (less than 30 minutes), making them possible candidates for many applications where fast recharge is important.

4. Design calculations indicate that the Li/Te cell with paste electrolyte can be expected to show a specific power in excess of 360 watt/lb and a specific energy of 80 watt-hr/lb, suggesting many possible applications, including special vehicle propulsion and energy storage.

#### Acknowledgment

It is a pleasure to thank Mr. J. Gerard for help with some of the experiments, and Drs. A. D. Tevebaugh, C. E. Johnson, and M. S. Foster for helpful discussions during the course of this work. Mr. B. S. Baker of the Institute of Gas Technology generously provided advice and materials on the preparation of paste electrolytes.

### References

1. R. Jasinski, "High-Energy Batteries", Plenum Press, New York (1967).
2. A. M. Moos and N. I. Palmer, in *Proc. 21st Ann. Power Sources Conf.*, PSC Publications Committee, Red Bank, New Jersey (1967).
3. H. N. Seiger, S. Charlip, A. E. Lyall and R. C. Shair, in *Proc. 21st Ann. Power Sources Conf.*, PSC Publications Committee, Red Bank, New Jersey (1967).
4. H. Shimotake and E. J. Cairns, Presented at the Intersociety Energy Conversion Engineering Conf., Miami Beach, August, 1967, in *Advances in Energy Conversion Engineering*, Amer. Soc. Mech. Eng., New York (1967), p. 951.
5. E. J. Cairns and H. Shimotake, Presented at Amer. Chem. Soc. Meeting, Chicago, September 1967, Abstr. No. L-70; See also *Preprints of Papers Presented to the Division of Fuel Chemistry 11*, No. 3, 321 (1967).
6. H. Shimotake, G. L. Rogers, and E. J. Cairns, Presented at Electrochem. Soc. Meeting, Chicago, October, 1967, Abstr. No. 18; See also *Extended Abstracts J-1 of the Battery Div.*, 12, 42 (1967).
7. R. A. Rightmire and A. L. Jones, in *Proc. 21st Ann. Power Sources Conf.*, PSC Publications Committee, Red Bank, New Jersey (1967).
8. H. A. Wilcox, in *Proc. 21st Ann. Power Sources Conf.*, PSC Publications Committee, Red Bank, New Jersey (1967).
9. H. Shimotake and E. J. Cairns, Presented at Electrochem. Soc. Meeting, Dallas, May, 1967, Abstr. No. 143; See also *Extended Abstrs. of the Industrial Electrolytic Div.*, 3, 4 (1967).
10. H. Shimotake and E. J. Cairns, Submitted for Presentation at the International Power Sources Symposium, Brighton, September, 1968.
11. G. H. J. Broers and M. Schenke, in "Fuel Cells", Vol. 2, G. J. Young, Ed., Reinhold, New York (1963).
12. B. S. Baker, L. G. Marianowski, J. Zimmer and G. Price, in "Hydrocarbon Fuel Cell Technology", B. S. Baker, Ed., Academic Press, New York (1965).
13. A. D. S. Tantram, A. C. C. Tseung, and B. S. Harris, in "Hydrocarbon Fuel Cell Technology", B. S. Baker, Ed., Academic Press, New York (1965).
14. C. E. Johnson, M. S. Foster, and M. L. Kyle, *Nuclear Appl.*, 3, 563 (1967).
15. C. E. Johnson, Submitted for Presentation at the San Francisco Meeting of The Amer. Chem. Soc., Apr., 1968.
16. M. S. Foster, S. E. Wood, and C. E. Crouthamel, *Inorg. Chem.*, 3, 1428 (1964).
17. M. S. Foster and C. C. Liu, *J. Phys. Chem.*, 70, 950 (1966).

Table I

Data for Battery Design Calculations

	<u>Li/Bi</u>	<u>Li/Te</u>
Open-circuit voltage, volts	0.8	1.7
Short-circuit current density, amp/cm <sup>2</sup> for electrolyte thickness 0.3 cm	1.8	2.2
for electrolyte thickness 0.1 cm	6.1	7.0
Cathode alloy, fully discharged composition, a/o Li	70	60
density, g/cm <sup>3</sup>	4.4	3.3
Anode metal density, g/cm <sup>3</sup>	0.53	0.53
Current efficiency, %	100	100
Cell partition thickness, cm/cell	0.1	0.1
Density of housing material, g/cm <sup>3</sup>	7.8	7.8
Density of paste electrolyte, g/cm <sup>3</sup>	3.0	3.0
Weight allowance for framing, terminals, etc. % (electrolyte + partition weight)	50	50

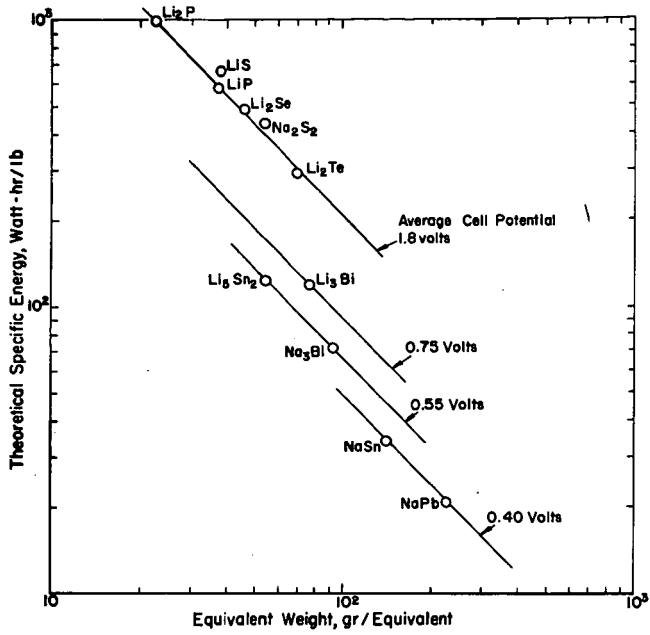


Fig. 1. Relationship between theoretical specific energy and equivalent weight

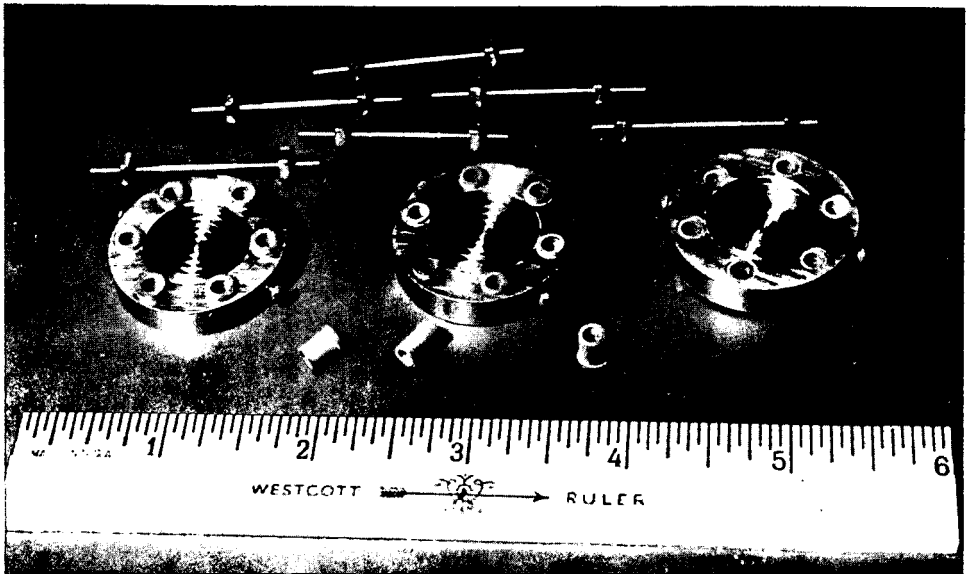


Fig. 2. View of lithium-bismuth-cell parts. Enough cell parts to make a two-cell battery are shown.

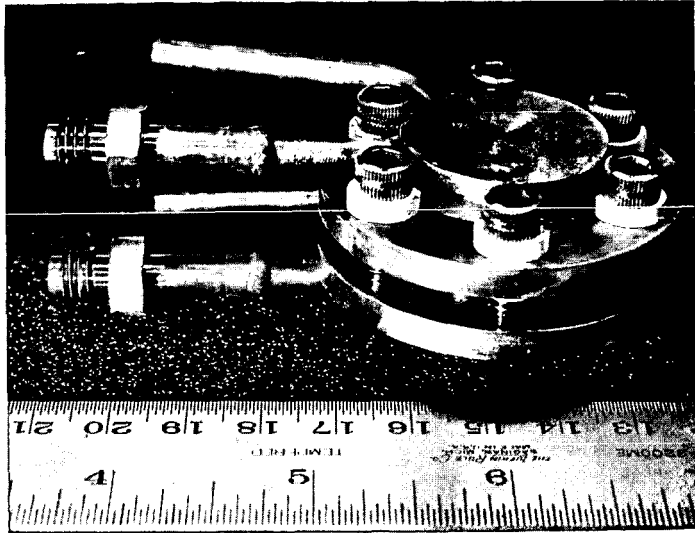


Fig. 3a. View of assembled lithium-tellurium cell

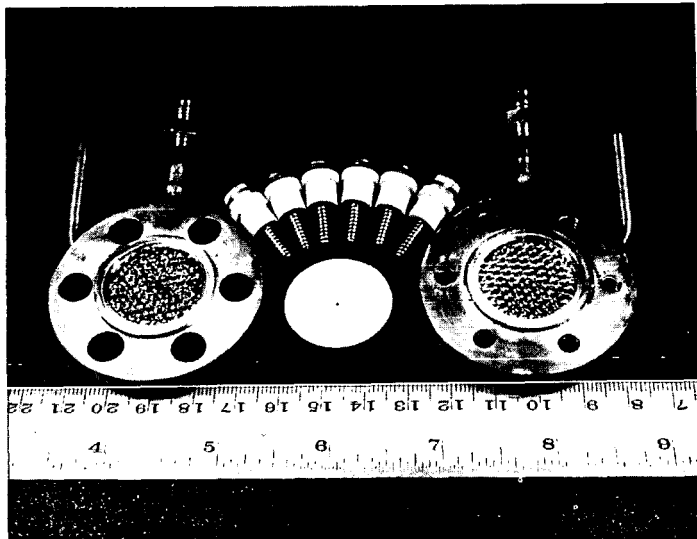


Fig. 3b. View of lithium-tellurium-cell parts



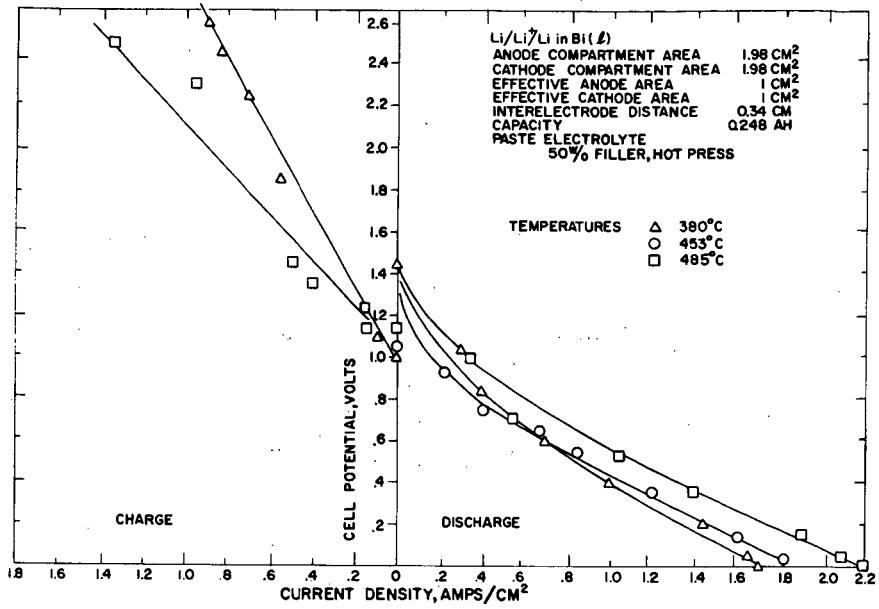


Fig. 4. Voltage-current density curves for a lithium-bismuth cell

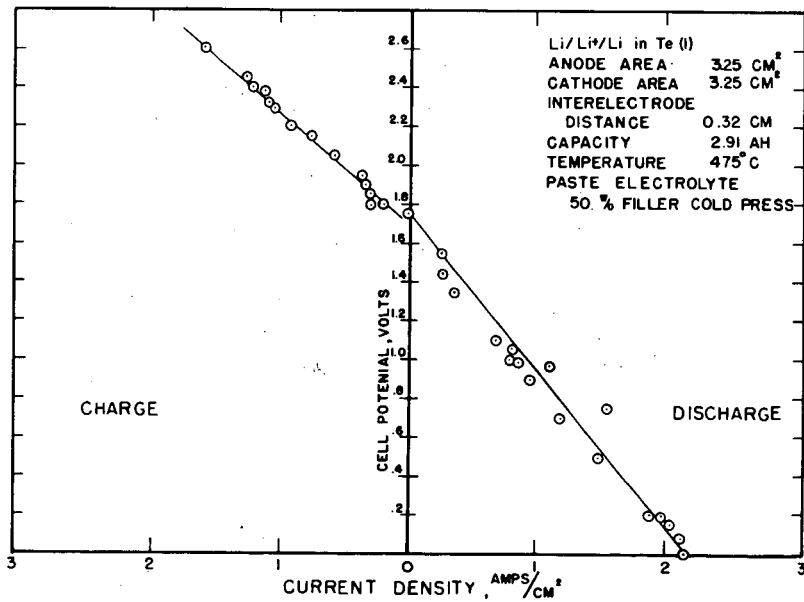


Fig. 5. Voltage-current density curves for a lithium-tellurium cell

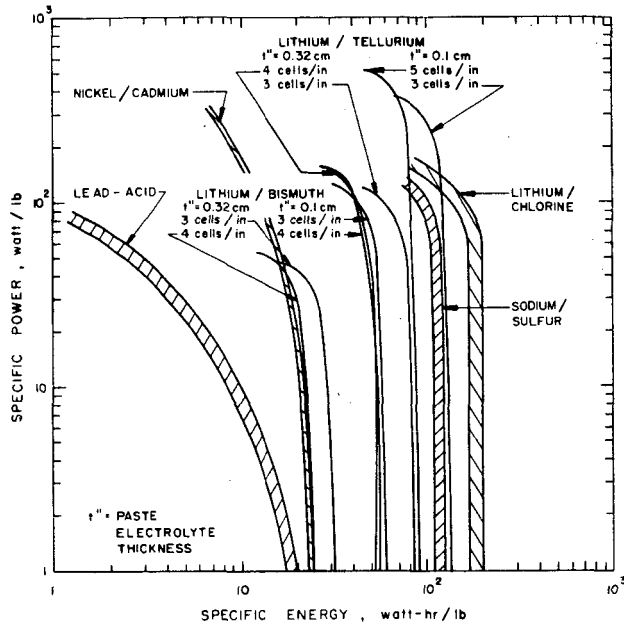


Fig. 6. Specific power-specific energy curves for some secondary batteries